

## CONTENTS

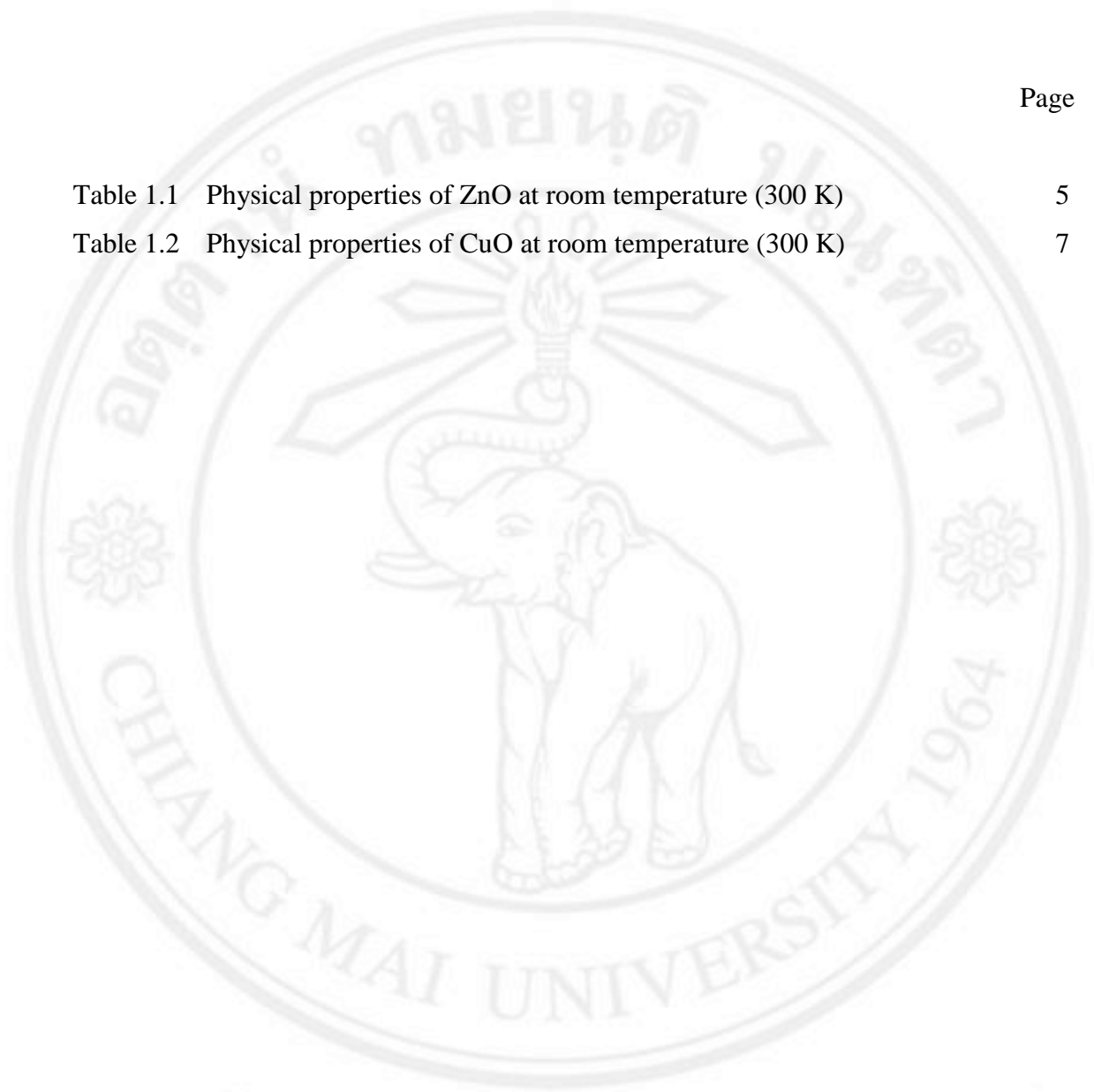
	Page
Acknowledgement	d
Abstract in Thai	e
Abstract in English	g
List of Tables	k
List of Figures	l
List of Abbreviations	p
Statement of Originality	q
Chapter 1 Introduction	1
1.1 Introduction	1
1.2 Transition Metal Oxides	2
1.3 Synthetic Method of TMOs	7
1.4 Application of TMOs	13
1.5 Literature Reviews	22
1.6 Research Objectives	28
Chapter 2 Experimental Procedures	29
2.1 Chemical reagents, Equipment and Instrument	29
2.2 Experimental Procedure	31
2.3 Characterization	35
2.4 Antibacterial Activity test	40
Chapter 3 Results and Discussion	41
3.1 Synthesis of zinc oxide by a hydrothermal method with different alkaline base solution	41

	Page
3.2 Synthesis of copper oxide by solution chemistry method at room temperature	71
Chapter 4 Results and Discussion	79
4.1 Conclusions	81
4.2 Suggestions	83
References	84
List of publications	95
Appendix A	96
Appendix B	101
Curriculum Vitae	134

ลิขสิทธิ์มหาวิทยาลัยเชียงใหม่  
Copyright© by Chiang Mai University  
All rights reserved

## LIST OF TABLES

	Page
Table 1.1 Physical properties of ZnO at room temperature (300 K)	5
Table 1.2 Physical properties of CuO at room temperature (300 K)	7



ลิขสิทธิ์มหาวิทยาลัยเชียงใหม่  
Copyright© by Chiang Mai University  
All rights reserved

## LIST OF FIGURES

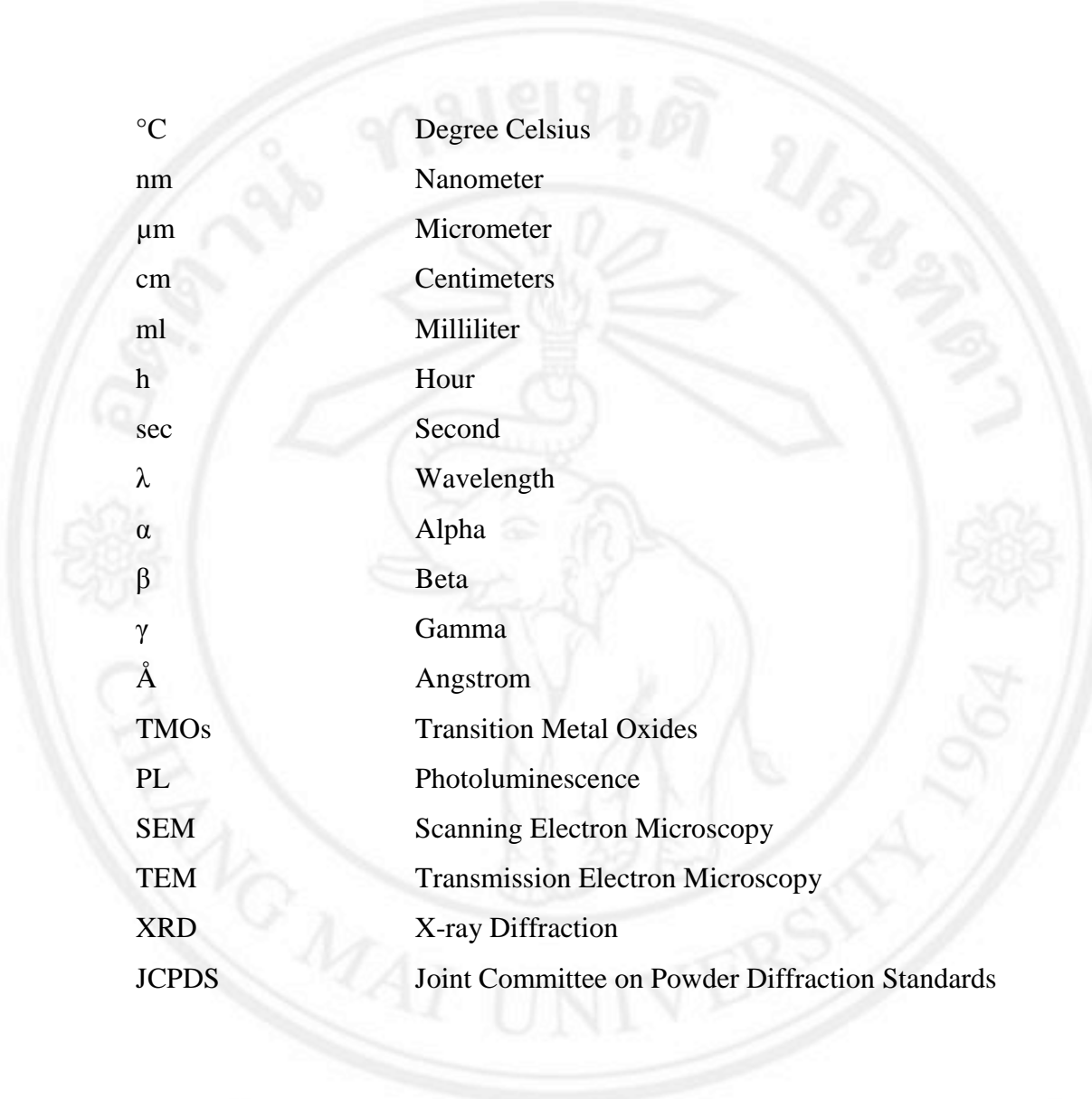
	Page	
Figure 1.1	Stick and ball representation of ZnO crystal structures: (a) cubic rock salt, (b) cubic zinc blende and hexagonal wurtzite.	3
Figure 1.2	ZnO has a noncentrosymmetric crystal structure that is made of alternate layers of positive and negative ions, leading to spontaneous polarization.	5
Figure 1.3	CuO monoclinic crystal structure.	6
Figure 1.4	Top-down and bottom up strategies.	8
Figure 1.5	Autoclave for used in Hydrothermal/Solvothermal method.	11
Figure 1.6	Schematic illustrations of a typical LIB and the electrochemical processes.	14
Figure 1.7	Schematic of the proposed sensing mechanism of NH <sub>3</sub> and NO <sub>2</sub> .	16
Figure 1.8	Schematic diagram of DSSC structures with different photoelectrodes for ZnO/CuO layer.	16
Figure 1.9	Photoconduction in a nanowire photodetector: (a) schematic of a nanowire photodetector. Trapping (b) photoconduction and (c) mechanism in ZnO nanowires.	17
Figure 1.10	Schematic of the principle of photocatalysis.	19
Figure 1.11	Diagram depicting the redox potentials of VB and CB as well as the band gap energies for various TMOs estimated at pH 7.	19
Figure 1.12	Schematic illustration of the antibacterial mechanism of CuO nanoparticles and the relative cellular structure of (a) Escherichia coli (Gram-negative) and (b) Staphylococcus aureus (Gram-positive).	21
Figure 2.1	Equipments for used.	30
Figure 2.2	Schematic diagram used for synthesized Zinc Oxide on Zn plate with NaOH by hydrothermal process.	31

	Page
Figure 2.3	Schematic diagram used for synthesized Zinc Oxide on Zn plate with LiOH by hydrothermal process. 32
Figure 2.4	Schematic diagram used for synthesized Zinc Oxide on Zn plate with NH <sub>4</sub> OH by hydrothermal process. 33
Figure 2.5	Schematic diagram used for synthesized Copper Oxide on Cu plate with NaOH by solution chemistry method 34
Figure 2.6	X-ray Diffractometer. 35
Figure 2.7	Raman Scattering Spectroscopy 36
Figure 2.8	Field Emission Scanning Electron Microscope 37
Figure 2.9	Transmission Electron Microscope 38
Figure 2.10	Photoluminescence Spectrophotometer 39
Figure 2.11	Schematic diagram used for test the antibacterial activity 40
Figure 3.1	XRD pattern of as-synthesized ZnO samples at difference pH synthesized by hydrothermal method. 42
Figure 3.2	SEM images of as-synthesized ZnO samples synthesized at pH (a) 9, (b) 10, (c) 11 and (d) 12 synthesized by hydrothermal method. 44
Figure 3.3	SEM images of as-synthesized ZnO samples at pH 12 with (a) 80°C, (b) 90°C, (c) 100°C and (d) 120°C synthesized by hydrothermal method. 46
Figure 3.4	TEM image, SAED pattern and HRTEM image of hexagonal pyramids ZnO nanorods. 45
Figure 3.5	schematic diagram of possible growth mechanism of hexagonal prism ZnO nanorods grow on Zn foil. 47
Figure 3.6	PL spectra of as-synthesized ZnO samples at difference pH synthesized by hydrothermal method. 49

	Page
Figure 3.7	XRD pattern of as-synthesized ZnO samples at difference weights of LiOH synthesized by hydrothermal method. 50
Figure 3.8	SEM images of ZnO samples using 0.10 g of LiOH synthesized by hydrothermal method.at 120 °C for (a) 1, (b) 6, (c) 18 and (d) 24 hrs. 51
Figure 3.9	SEM images of XRD pattern of as-synthesized ZnO samples synthesized by hydrothermal method.at 120 °C for 24 h using a) 0.05, (b) 0.20, (c) 0.30 and (d) 0.40 g of LiOH. 53
Figure 3.10	TEM image and SAED pattern and HRTEM image of hexagonal pyramids ZnO nanorods. 55
Figure 3.11	TEM image and SAED pattern and HRTEM image of hexagonal pyramids ZnO nanorods. 56
Figure 3.12	schematic diagram of possible growth mechanism of hexagonal prisms and hexagonal pyramids ZnO microstructures grow on Zn foil. 58
Figure 3.13	PL spectra of as-synthesized ZnO samples at difference weights of LiOH synthesized by hydrothermal method. 60
Figure 3.14	XRD patterns of ZnO synthesized in NaOH, LiOH and NH <sub>4</sub> OH alkaline precursor solutions. 61
Figure 3.15	Raman spectra of ZnO synthesized in NaOH, LiOH and NH <sub>4</sub> OH alkaline precursor solutions. 63
Figure 3.16	SEM images of ZnO synthesized in (a) NaOH, (b) LiOH and (c) NH <sub>4</sub> OH alkaline precursor solutions. 64
Figure 3.17	TEM images, SAED patterns and simulated patterns of ZnO synthesized in (a) NaOH, (b) LiOH and (c) NH <sub>4</sub> OH alkaline precursor solutions. 65
Figure 3.18	A schematic diagram for formation mechanisms of rod-like, pencil-like and star-like ZnO products. 66

	Page
Figure 3.19	PL spectra of ZnO synthesized in NaOH, LiOH and NH <sub>4</sub> OH alkaline precursor solutions. 67
Figure 3.20	Effect of E. Coli in activation for ZnO synthesized in different alkaline precursor solutions: (a, d) LiOH, (b, e) NaOH and (c, f) NH <sub>4</sub> OH; (a-c) before and (d-f) after incubation. 68
Figure 3.21	Effect of S. aureus in activation for ZnO synthesized in different alkaline precursor solutions: (a, d) LiOH, (b, e) NaOH and (c, f) NH <sub>4</sub> OH; (a-c) before and (d-f) after incubation. 69
Figure 3.22	Comparative analysis of zone diameter of ZnO with different morphologies on E. Coli and S. aureus. 70
Figure 3.23	A schematic diagram of antibacterial mechanism. 70
Figure 3.24	XRD patterns of CuO thin films grown on Cu foils by wet chemical method at room temperature for 1, 2 and 3 weeks. 71
Figure 3.25	SEM images of thin films grown on Cu-foils by wet chemical method at room temperature for (a-i) 3, 5, 7, 9, 12, 14, 16, 19 and 21 days, respectively. 72
Figure 3.26	(a) TEM image and (b) SAED pattern of an assembly of nanospindles grown on copper foil by wet chemical method at room temperature for 2 weeks. (c, d) The simulated pattern and unit cell of a spindle. 73
Figure 3.27	Different stages for the formation of solid thin films on copper foils. 75
Figure 3.28	PL spectra of thin films grown on Cu foils by wet chemical reactions at room temperature for 1, 2 and 3 weeks. 77
Figure 3.29	Antibacterial activity of CuO thin films for (a, b) S. aureus, and (c, d) E. coli. (a, c) before and (b, d) after testing. 78

## LIST OF ABBREVIATIONS

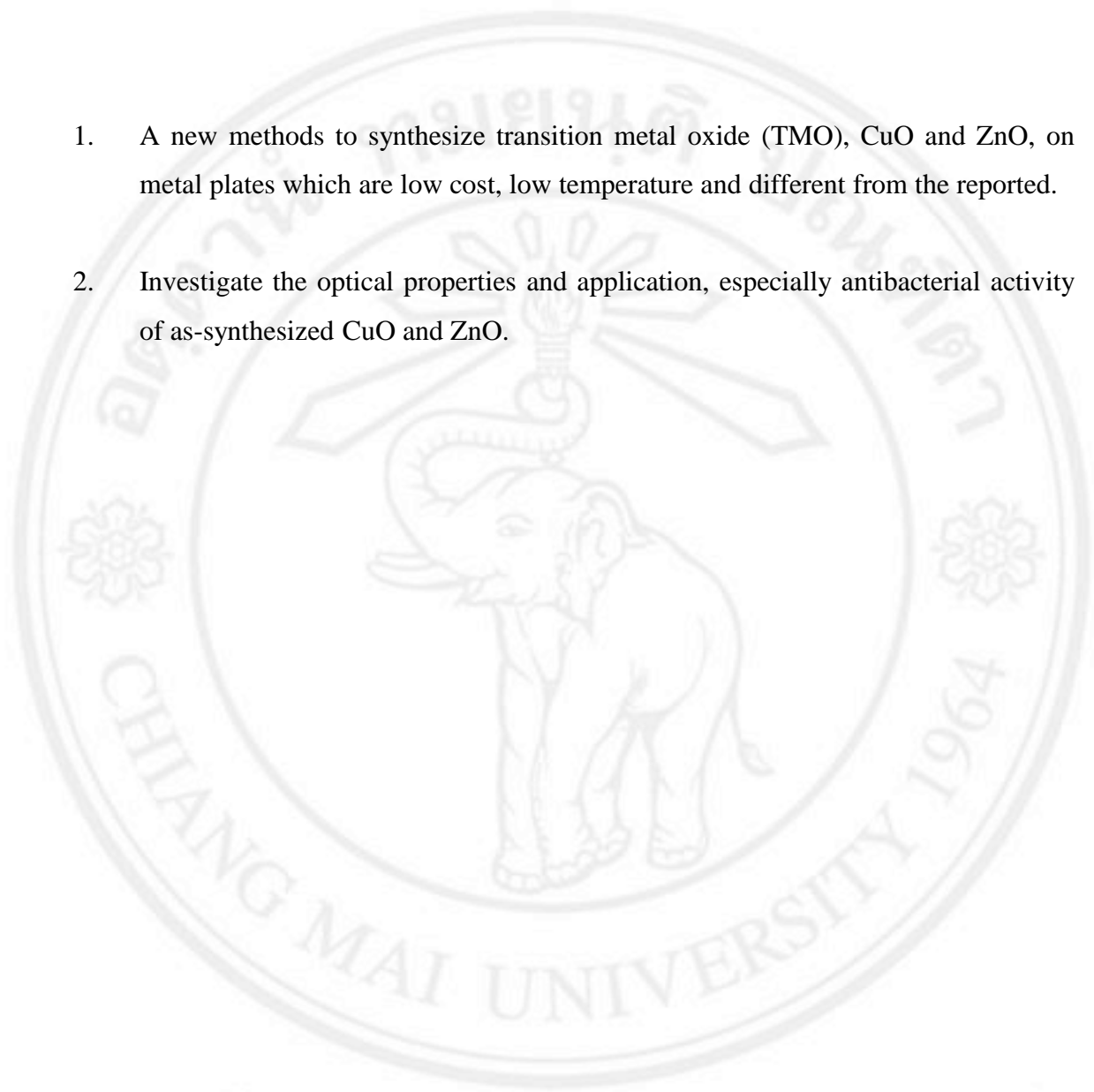


°C	Degree Celsius
nm	Nanometer
μm	Micrometer
cm	Centimeters
ml	Milliliter
h	Hour
sec	Second
λ	Wavelength
α	Alpha
β	Beta
γ	Gamma
Å	Angstrom
TMOs	Transition Metal Oxides
PL	Photoluminescence
SEM	Scanning Electron Microscopy
TEM	Transmission Electron Microscopy
XRD	X-ray Diffraction
JCPDS	Joint Committee on Powder Diffraction Standards

ลิขสิทธิ์มหาวิทยาลัยเชียงใหม่  
Copyright© by Chiang Mai University  
All rights reserved

## STATEMENT OF ORIGINALITY

1. A new methods to synthesize transition metal oxide (TMO), CuO and ZnO, on metal plates which are low cost, low temperature and different from the reported.
2. Investigate the optical properties and application, especially antibacterial activity of as-synthesized CuO and ZnO.



ลิขสิทธิ์มหาวิทยาลัยเชียงใหม่  
Copyright© by Chiang Mai University  
All rights reserved